JOURNAL OF MATERIALS SCIENCE 22 (1987) 1365–1373

Plasticity by martensite transformations in cobalt base metallic glasses?

T. ERTÜRK*, A. S. ARGON
Department of Mechanical Engineering, Massachusetts Institute of Technology, Cambridge, Massachusetts 02139, USA

The possibility of mechanical coupling to applied stresses of martensitic transformations in $Co_{80}Nb_{14}B_6$ and $Co_{84}Nb_{10}B_6$ metallic glasses reported by O'Handley and co-workers in the temperature range 295 to 473 and 513 K, respectively, was investigated. Since martensitic transformations strongly couple with externally applied shear stresses, internal friction scans and plastic resistance measurements in both tension and plane-strain compression were carried out in thermal cycles in the same temperature range, complemented with differential scanning calorimetry observations. No transformation plasticity was detected in these glasses as internal friction showed no peaks, DSC showed no heat evolution or absorption, and the temperature dependence of flow stress exhibited a monotonically decreasing behaviour.

1. Introduction

Transformation plasticity involves production of strain resulting from phase transformations occurring under stress. Although a variety of transformations, such as diffusional allotropic transformations and precipitation reactions, are known to produce transformation plasticity, it is the martensitic transformations under stress that give the largest strains, and thus form the basis for practical applications, such as enhanced uniform ductility influencing sheet formability, and toughness in metastable austenitic steels. It should be noted here that properties obtained from transformation plasticity are based mainly on the transformation itself rather than on the transformation product. The latter can separately influence performance in the form of enhanced deformation resistance.

Martensitic transformations occurring upon cooling without stress can be regarded as a kind of spontaneous, randomly oriented plastic deformation driven by internal chemical free energy changes as they take place through a displacive or shear process, leading to an invariant-plane strain on a macroscopic scale. When a martensitic transformation is coupled with an externally applied stress, biasing by the latter of the martensitic orientation variants along with biasing of accommodation slip leads to the development of large-strain transformation plasticity.

Transformation plasticity alters the shape of the true stress–true strain curve from a conventional downward configuration of negative curvature to one of positive curvature by a "dynamic softening" effect of the transformation as a deformation mechanism at low strains, and a "static hardening" contribution of the transformation product in the later stages. The positive curvature resulting from this combined effect represents an ideal behaviour for securing macroscopic flow instability [1]. This permits dramatic enhancement of uniform ductility, as mentioned above, and represents the most well-established application of transformation plasticity. In transformation toughening of metastable austenitic steels, including the newly-developed dual phase steels containing small amounts of retained austenite, toughening is thought to be affected by flow-delocalization and transformation dilatancy phenomena associated with the concurrent transformation.

Recently, O'Handley and co-workers [2–7] presented experimental evidence of a special type of hysteresis behaviour in the eutectic $Co_{80}Nb_{14}B_6$ metallic glass when cycled under an applied magnetic field of 1000 Oe between room temperature and 473 K, somewhat analogous to the hcp–fcc (ε–γ) martensitic transformation in cystalline cobalt and cobalt-rich alloys. Specifically, they observed a scan rate-dependent thermomagnetic hysteresis of $\Delta T = 100$ K, centred at $T_0 = 381$ K. No hysteresis was detected upon heating and cooling this material in saturation magnetic fields. The thermomagnetic hysteresis loop for a second composition, $Co_{84}Nb_{10}B_6$, containing small amounts of microcrystallites (~ 10 vol %), did not however close at room temperature, and no sub-ambient measurements were made. The transformation was distinguished from structural relaxation phenomena in metallic glasses by its kinetics, which were described by an activation energy which decreased with an increasing temperature difference $|T-T_0|$, above or below T_0. Proposing that these observations indicated a reversible martensitic type transformation in these metallic glasses, a model was proposed by these authors for the local shear transformation involving clusters of trigonal (low temperature) and octahedral (high temperature) symmetry.

Although metallic glasses are capable of undergoing extensive plastic deformation with no hardening, flow

*Visiting Associate Professor in the Department of Mechanical Engineering (1984–6), on leave from Middle East Technical University, Ankara, Turkey.

0022–2461/87 $03.00 + .12

at temperatures below $\sim 0.71\,T_g$ is in the form of intense shear bands, rendering these materials plastically unstable with an apparent macroscopic "brittleness" and low toughness. Since the structure is not altered significantly by deformation, it has been proposed that the retained flow dilation (local increase in free volume) resulting in shear strain induced reduction of deformation resistance is responsible for the localization of flow [8]. A martensitic transformation under stress in an amorphous structure can provide a finite macroscopic strain, without the attendant deleterious flow dilation and with the possible beneficial effects of only a finite transformation-induced dilatancy, as opposed to undesirable limitless shear-induced dilatancy. In addition, the static hardening effect of the transformation product may enhance flow stability.

The goal of the present investigation has been to explore the possible mechanical coupling of the hysteresis phenomena observed in the $Co_{80}Nb_{14}B_6$ amorphous alloy by O'Handley and co-workers [2–7], and to determine whether or not they involved martensitic transformations. This, in turn, should assist in the determination of the possible stress and temperature regimes where such a transformation could be utilized to impart uniform ductility and toughness to this material.

2. Background

When a martensitic transformation is part of an imposed deformation, the temperature dependence of the yield stress assumes the shape of an inverted V. This is illustrated schematically in Fig. 1 for metastable austenitic steels, where the heterogeneous shear transformations nucleate under stress at existing sites, assisted by the thermodynamic effect of applied stress below the M_s^σ temperature and by strain-induced nucleation on new sites, created by plastic strain above M_s^σ [9]. At the M_s temperature, spontaneous transformation on existing sites is triggered by chemical free energy changes alone. The critical applied stress producing yielding through the start of martensitic transformations increases linearly with increase in temperature between M_s and M_s^σ [10–13]. This is expected because the chemical driving force decreases linearly with increase in temperature above M_s. Above M_s^σ, the yield stress of the parent phase is reached before sufficient mechanical contribution of the thermodynamic driving force is available for the onset of the martensitic transformation. Between M_s^σ and M_d, new potent nucleation sites created by plastic deformation trigger strain-induced nucleation and a temperature dependence of yield stress with positive curvature is obtained. Clearly, a discontinuous (V-shaped) temperature dependence of the yield stress of a metallic glass would be strongly indicative of a mechanical coupling of the martensitic transformation to the applied stress, and qualify the observations reported by O'Handley and co-workers [2–7] to be as such.

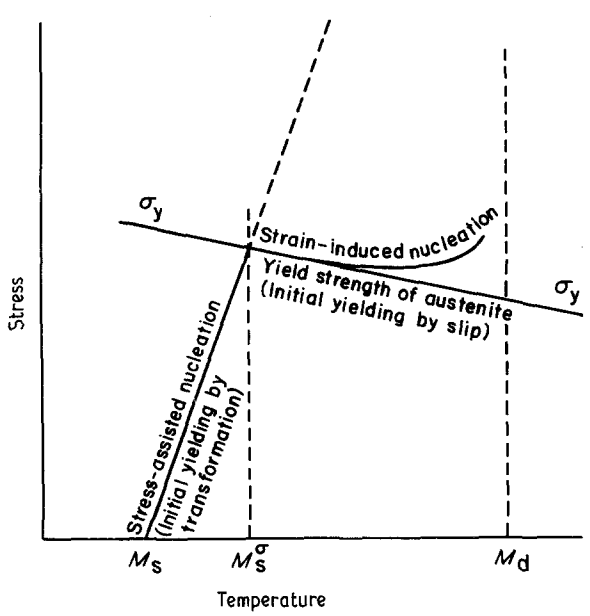

Figure 1 Temperature dependence of yield stress in the presence of transformation plasticity. Between M_s^σ and M_s temperatures, transformation induced yielding occurs at diminishing stresses [9].

It is now well established that in metallic glasses, inelastic flow arises from shear transformations in regions of excess free volume [8] or in clusters of atoms with large atomic level internal stresses [14] as they undergo internal atomic rearrangements. Internal friction in the elastic range at strain levels of about 1% of the yield strain, provides a sensitive and non-invasive mechanical probe to the distributed nature of the shear relaxations in the glass structure and is used extensively for this purpose. Since martensitic shear transformations can strongly couple with externally applied shear stresses, this technique should also be sensitive to reversible martensitic shear transformations of the type proposed by O'Handley and co-workers [2–7] to explain their magnetic hysteresis observations. Specifically, a strong peak should be observed in the temperature range reported for the cobalt–base glasses, superimposed on the background damping due to the usual localized shear transformations at large free volume sites mentioned above, provided that such martensitic transformations do not require a high stress to initiate them.

In the present study, both internal friction and flow stress measurements were included to detect the presence of martensitic transformations, in case they indeed require a high stress to initiate them.

3. Experimental procedure

3.1. Materials

Melt-spun $Co_{80}Nb_{14}B_6$ and $Co_{84}Nb_{10}B_6$ amorphous alloys, having reduced metalloid content, exhibiting good ductility [15] and excellent magnetic properties in the crystallized state, were kindly supplied in the form of continuous ribbons by R. C. O'Handley of the Department of Materials Science and Engineering, Massachusetts Institute of Technology, USA. The thickness of the ribbons were determined to be 25 and 28 μm, respectively, using light microscopy. Similarly, the widths were 0.83 mm for the Co_{80} ribbon, and 1.04 mm for the Co_{84} glass. Ribbon widths showed little variation along the length of the specimens. The thickness in both alloys, however, showed irregularities in the form of short- and long-wavelength

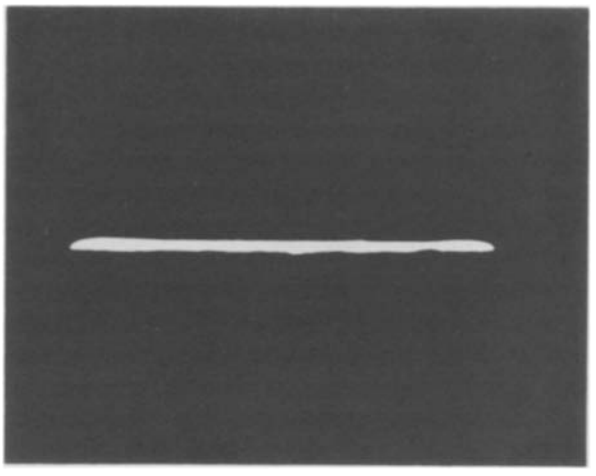

Figure 2 Cross-section of $Co_{80}Nb_{14}B_6$ glass. The width of the ribbon is 0.83 mm.

roughness in the width direction; a cross-section of the Co_{80} alloy is shown in Fig. 2. Samples, 3 mm wide, of the same compositions, rapidly solidified under identical conditions, were also obtained from B. W. Corb of the Institute for Physics, University of Basel, Switzerland.

Differential scanning calorimetry (DSC) was used to determine the structural transition temperatures in both alloys. The DSC examination indicated no heat evolution during cycling between room temperature, and 473 and 513 K for the Co_{80} and Co_{84} glasses, respectively. No glass transition or other significant transition could be detected for either alloy prior to crystallization. DSC showed a single and broad peak with the onset of crystallization at 743 and 713 K, respectively, for these two alloys, at a heating rate of 20 K min^{-1}.

Hardness measurements on the as-received ribbons were performed using a Leco M-400 micro-hardness tester equipped with a Vickers diamond pyramid indenter. Both 50 and 100 g indentation loads were used with no difference in results. The ribbons were attached at the ends to glass plates by adhesive tapes, to prevent sliding. All indentations were made on the original surfaces of the ribbons, so as not to alter the state of the material by metallographic polishing. Indentations were made both on top (shiny) and bottom (dull) surfaces of the ribbons, resulting in a substantial difference in hardness values. Top-surface hardnesses were determined from at least 10 indentations, as 9.20 and 8.65 GPa for the Co_{80} and Co_{84} glasses, respectively. The hardness measurement of the dull (bottom) side was hampered by the roughness of this surface, which was in contact with the quenching wheel; only a small percentage of the many indentations on the rough surfaces were of readable quality. Nevertheless, a bottom-surface hardness of approximately 9.75 GPa for the Co_{80} glass and 9.15 GPa for the Co_{84} glass was estimated from such measurements. Thus, in both glasses, the hardness of the dull surface was about 5 to 6% higher than that of the shiny surface. The coefficient of variation of the hardness of the shiny side was 0.05. All indentations on the shiny sides in both glasses were decorated with so-called "coronets", which are indicative of amorphous structure.

3.2. Electron microscopy

The microstructural characterization of the as-received material and several Co_{80} ribbons aged to crystallization was performed by transmission electron microscopy using a JEOL 200 CX microscope. Specimens of 3 mm width were thinned by electrolytic polishing in a solution of 10% $HClO_4$ and 90% CH_3OH at 228 K and 25 V. Most TEM observations were made in the dark field mode.

3.3. Internal friction

An inverted torsion pendulum was used to obtain internal friction spectra in thermal cycling between room temperature, and 473 and 513 K for the $Co_{80}Nb_{14}B_6$ and $Co_{84}Nb_{10}B_6$ glasses, respectively, with and without applied saturation magnetic fields, and utilizing different frequencies near 0.3 Hz in a vacuum of 10^{-5} torr. The logarithmic decrement δ was measured from the decay of the peak velocity at zero amplitude using the equation

$$\delta = \frac{1}{n} \ln \left(\frac{V_0}{V_n} \right) \tag{1}$$

where V_0 is the peak velocity at the chosen initial time $t = 0$, and V_n is the zero amplitude velocity after n integral periods, i.e., after a time $t = n\tau$. This is equivalent to the measurement of δ from the decay of the amplitude of free oscillations.

The test equipment was comprised of an optical lever system consisting of a mirror mounted on the upper specimen holder, a projector lamp, and two sensitive photocells 12 mm apart. The output of the photocells was recorded using a high speed chart recorder, and the velocity decay V_0/V_n was determined from measurements of these outputs using a toolmaker's microscope. By changing the moment of inertia of the torsion pendulum, oscillation frequencies between 0.15 and 0.42 could be obtained.

Several internal friction scans at a heating rate of 5 K min^{-1} were carried out up to the crystallization temperature. Logarithmic decrement measurements of 1 min duration were made every 20°, during which the temperature was held constant. The temperature variation along the 54 mm length of the specimen was within 2 K.

A small tensile stress of about 1 MPa was applied to the specimens during internal friction scans. This is about one third of the stress to cause creep near the crystallization temperatures. The maximum surface shear strain at the start of free oscillation was about 10^{-5}. This is about 1% of the elastic yield strain at the highest temperatures, and demonstrates the non-invasiveness of the technique.

Shear moduli of the amorphous alloys as a function of temperature were calculated from the measured oscillation frequencies. To this end, the moment of inertia of the torsion pendulum was determined using a standard nickel specimen of known shear modulus [15].

3.4. Flow stress measurements

The possibility of transformation plasticity in the eutectic $Co_{80}Nb_{14}B_6$ glassy alloy was investigated

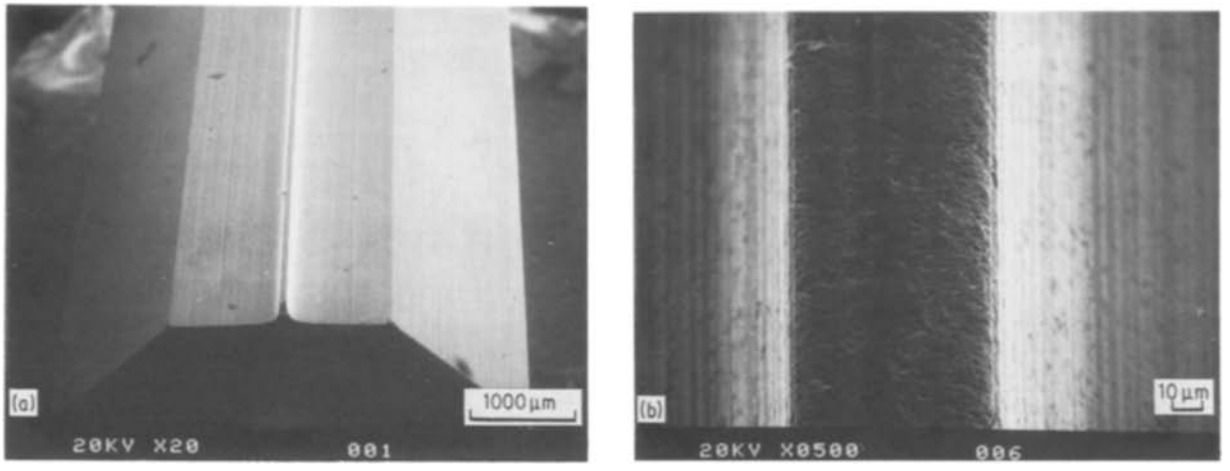

Figure 3 Tungsten carbide die used in the plane-strain compression tests. (a) The width of the die is 4.8 mm, and (b) the width of the indenting edge is 70 μm.

through flow stress measurements in both tension and plane-strain compression. Tension tests were conducted in an Instron machine using special friction grips at an initial strain rate of $4 \times 10^{-3}\,\mathrm{sec}^{-1}$, in an Instron environmental chamber filled with purified argon gas. Fifteen specimens were heated to 473 K and tested at this temperature. The remainder of the test program involved heating the specimens to 473 K, then cooling and testing five specimens at 20 K intervals. Thus, conditions were created for the material first to be "transformed" into a more stable high temperature (presumably with octahedral symmetry) phase, then yield stress measurements were made to detect the existence of any stress-assisted transformations. In the case of transformation plasticity, as noted in Section 2, the yield stress should diminish toward zero, beginning at the M_s^σ temperature.

The Young's modulus of the ribbon at different temperatures was estimated by first testing tungsten wires of known modulus to account for the compliance of the testing system [15]. Although considerable scatter was found in the measurements (a coefficient of variation of 0.1), the results were validated using the pulse induced resonance technique [16].

A complementary set of measurements was carried out in plane-strain compression over the same temperature range for this amorphous ribbon. Plane-strain compression tests were performed because below $\sim 0.7\,T_g$, in the inhomogeneous flow region, metallic glasses are prone to intense shear localization and a plastic instability induced premature failure, with negligible homogeneous plastic flow [17]. To this end, precision machined, 70 μm wide WC platens, depicted in Fig. 3, were attached to a small precision compression jig in the form of engaged double stirrups, all immersed in an oil bath. Because of the geometry, hardness, and roughness differences between the shiny and dull surfaces of the ribbons, equal indentations on both sides could not be obtained using single ribbons. Instead, the ribbons were folded over around the dull side, exposing the shiny faces to indentation. This resulted in a more favourable deformation zone geometry, i.e., ratio of indenter width to specimen thickness, thereby decreasing further friction effects [18]. The tests were conducted at a cross-head speed of $0.005\,\mathrm{mm\,min}^{-1}$, giving an initial strain rate of $1.7 \times 10^{-3}\,\mathrm{sec}^{-1}$.

4. Results

4.1. Electron microscopy

TEM studies showed that both the Co_{80} and Co_{84} glasses were amorphous in the as-cast state, with no phase separation. Typical dark field TEM images of the alloys, with the corresponding selected area diffraction patterns, are given in Figs 4 and 5. The grainy pattern seen in Figs 4 and 5 is characteristic of glassy materials. In contrast to the observations of O'Handley and co-workers [2–7], these micrographs and diffraction patterns show single phase, nearly-perfect glassy structures for the as-received melt-spun alloys.

A number of Co_{80} specimens were aged at 668 K ($0.9\,T_c$) at one hour intervals up to 4 h. The microstructure and selected area electron diffraction pattern of a sample aged 4 h at this temperature are shown in Fig. 6. This dark field TEM image revealed the presence of randomly oriented, large white areas, identified as cobalt microcrystals embedded in an amorphous matrix. The electron diffraction pattern consisted of diffuse scattering around the bright central spot, characteristic of the amorphous structure. The outer diffraction rings, however, contained distinct maxima indicating partial crystallinity. TEM studies showed that in the Co_{80} glass, crystallization starts after approximately 3 h of ageing at 668 K.

4.2. Internal friction

Internal friction spectra without applied saturation magnetic fields at a nominal frequency of 0.15 Hz, in thermal cycles between room temperature and 473 and 513 K for the Co_{80} and Co_{84} glasses, respectively, are presented in Fig. 7. These results show low, temperature independent logarithmic decrements of around 1.7×10^{-3}, exhibiting no peaks. Repeating these experiments under an applied saturation magnetic field did not change the level of the logarithmic decrements in either alloy in a detectable way. It is, however, to be noted that the low level of background damping is probably equipment limited, and that it most probably results from an irreducible level of gripping friction.

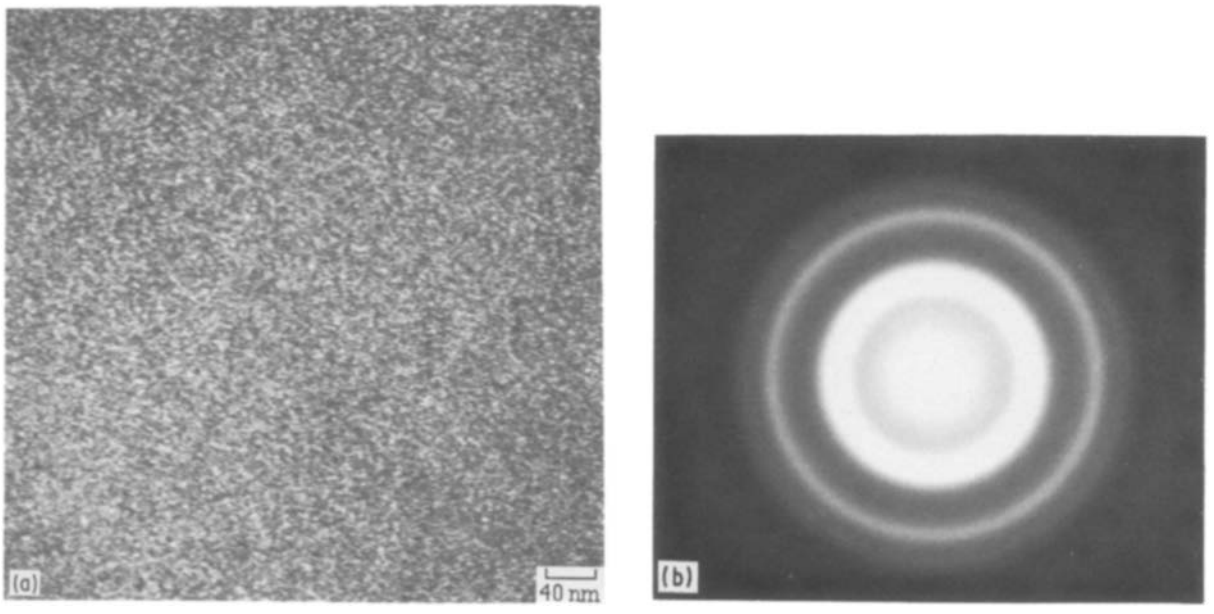

Figure 4 (a) Dark field TEM micrograph and (b) corresponding selected area diffraction pattern of $Co_{80}Nb_{14}B_6$ metallic glasses in the as-cast state. The salt and pepper appearance is characteristic of these alloys.

Internal friction scans carried out with and without applied saturation magnetic fields up to the crystallization temperatures of both materials showed a conventional behaviour observed in many other glassy metallic systems; i.e., low fractional energy loss per cycle at an almost constant level up to about $T_c - 200\,K$, followed by a near exponential increase up to T_c, complete with regular frequency shift effects, as given in Fig. 8. Fig. 9 illustrates internal friction spectra for the Co_{80} alloy at 0.15 Hz, in the as-received condition and aged at 668 K for 1 and 2 h. Ageing this alloy at the same temperature for 2.5 h during which no crystallization occurs, gave the same internal friction spectra as that for 2 h ageing, indicating establishment of a quasi-equilibrium structure in the glass [19].

4.3. Elastic constants

Pendulum frequencies at constant settings of inertia in internal friction experiments involving thermal cycling showed smooth and gradual variations, indicating only slowly varying shear moduli, as shown in Fig. 10.

Young's modulus and Poisson's ratio as a function of temperature for the Co_{80} alloy are presented in Fig. 11. The temperature dependence of the Young's modulus is similar to that of the shear modulus given in Fig. 10, yielding a Poisson's ratio of 0.32, which remains constant over the temperature range.

4.4. Plastic resistance

Fig. 12 shows the nominal stress–strain curve in plane-strain compression for the $Co_{80}Nb_{14}B_6$ glass,

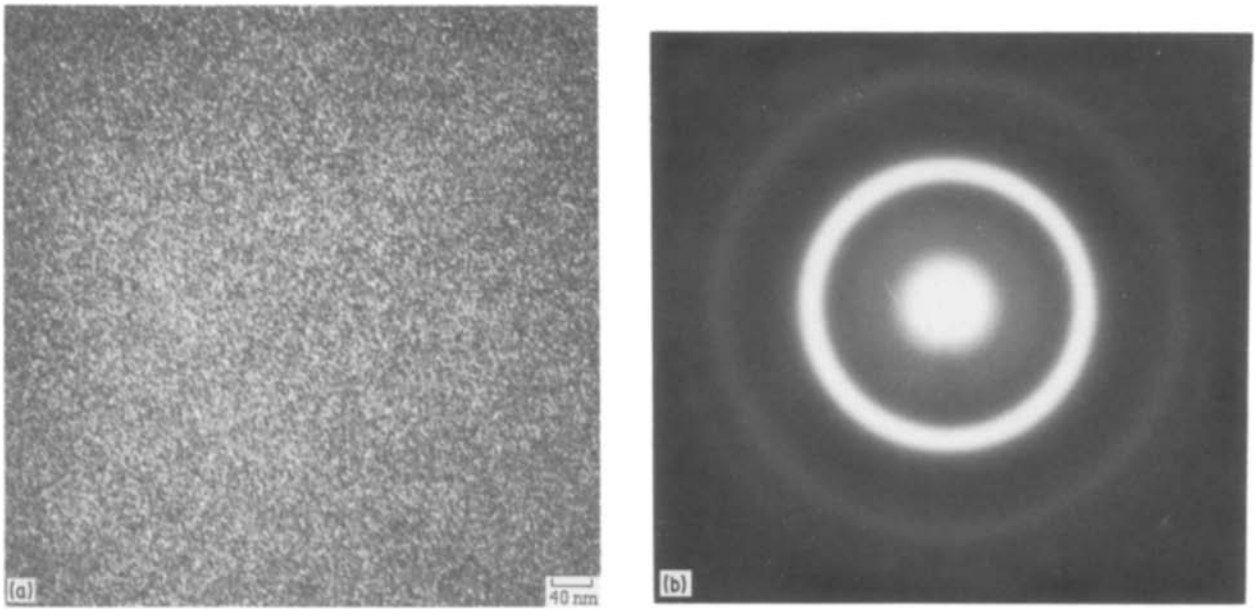

Figure 5 (a) Dark field TEM micrograph and (b) corresponding selected area diffraction pattern of melt spun $Co_{84}Nb_{10}B_6$ glass. The grainy pattern is characteristic of these alloys.

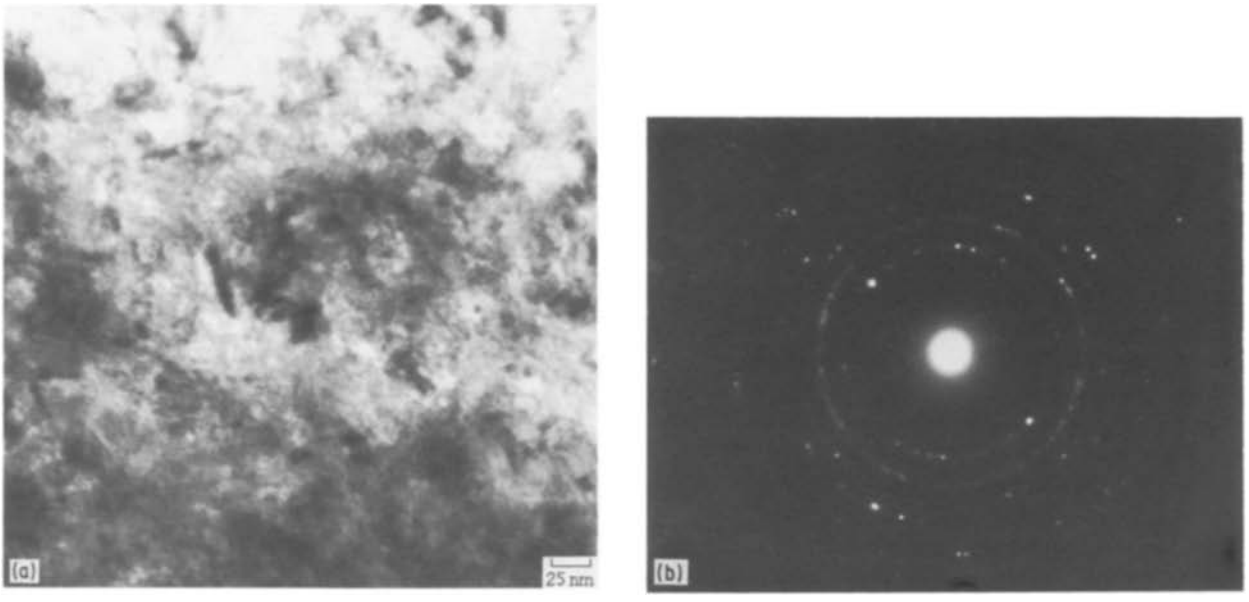

Figure 6 (a) Dark field TEM micrograph and (b) corresponding selected area diffraction of partially crystalline $Co_{80}Nb_{14}B_6$ alloy aged 4 h at 668 K (0.9 T_c). White areas are cobalt microcrystals embedded in an amorphous matrix.

obtained at 295 K from the recorder chart; the broken line indicates the compliance of the testing machine. In tension, specimens failed by inhomogeneous plastic flow, remaining elastic up to fracture at any temperature, even at strain rates as low as $8 \times 10^{-5}\,sec^{-1}$. In plane-strain compression, on the other hand, extensive serrated plastic flow due to repeated shear band initiation [20] occurred prior to final shear failure, Fig. 12. The serrations had amplitudes ~1% of the applied load at room temperature, but increased to ~5% of the applied load at 473 K. In all cases, flow stresses were determined from the maximum loads. Subtracting the machine compliance, obtained without specimens between the indenter dies, indicated up to ~25% plastic strain, in serrated flow, before the final unstable separation.

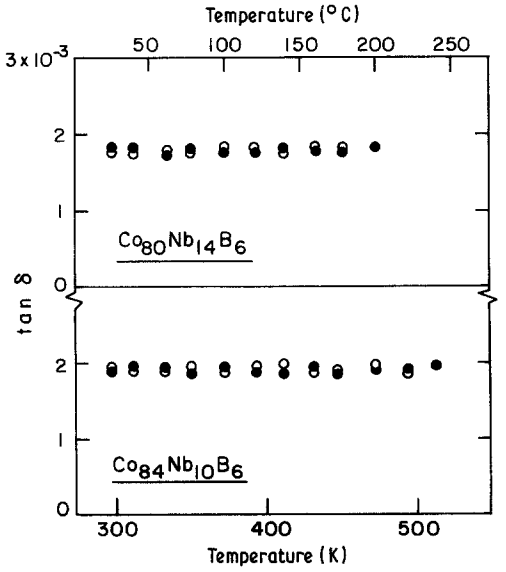

Figure 7 Internal friction scans at a nominal frequency of 0.15 Hz for $Co_{80}Nb_{14}B_6$ and $Co_{84}Nb_{10}B_6$ metallic glasses in thermal cycles between room temperature and 473 and 513 K, respectively, without applied saturation magnetic fields. No detectable change in the spectra was observed in repeating the experiments under applied saturation magnetic fields. ○, heating; ●, cooling.

Flow stresses in tension and plane-strain compression, corrected for plain-strain constraint, up to 473 K are presented in Fig. 13. Yield stresses obtained from tension tests are approximately 5% lower than the plane-strain compression test data. The scatter in the plane-strain compression measurements with a coefficient of variation of 0.03 was quite small; scatter was twice this value in simple tension.

5. Discussion

Clearly, the internal friction behaviour exhibited by the Co_{80} alloy, its frequency dependence and the effects of ageing, as shown in Figs 8 and 9, is worthy of a more detailed investigation of the distributed nature of shear relaxations at large free volume sites or at large residual internal atomic level stresses. However, since the goal of the present study was to explore the possibility of transformation plasticity in the glass, a more detailed study of structural relaxation kinetics was not carried out.

Serrations and the attendant increase in stress level in the early portions of the stress–strain curve in plane

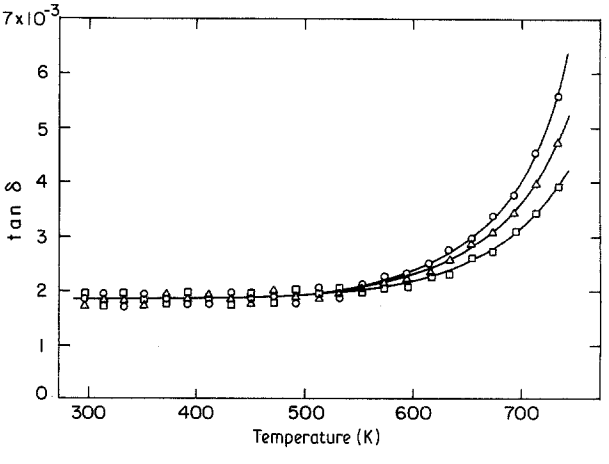

Figure 8 Internal friction spectra for the $Co_{80}Nb_{14}B_6$ glass between room temperature and crystallization temperature (743 K). Frequency: ○, 0.15; △, 0.24; □, 0.42 Hz.

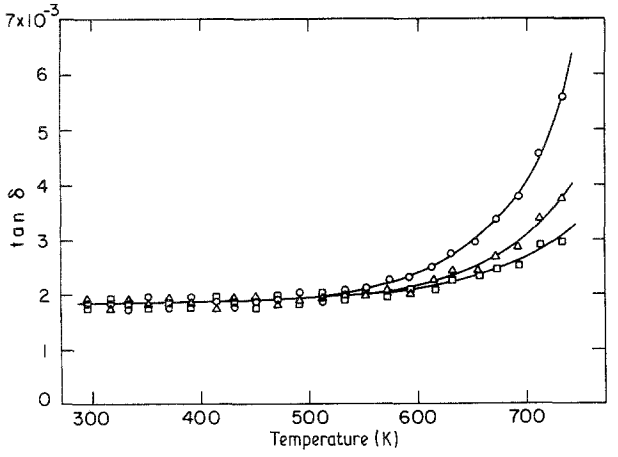

Figure 9 Effect of ageing at 668 K on the internal friction spectrum of $Co_{80}Nb_{14}B_6$ glass at a nominal frequency of 0.15 Hz. The lowest curve corresponds to an established quasi-equilibrium structure before the onset of crystallization. ○, As-quenched; △, aged 1 h at 668 K; □, aged 2 h at 668 K.

strain compression are attributed to the irregular geometry of the folded ribbons (see Fig. 2). Early jerky flow should be due to early shear banding caused by the short- and long-wavelength roughness of the dull and shiny surfaces of the two folded sheets, respectively, along with indentations caused by the surface roughness of the dies. It was thought that any attempt to flatten the surfaces, including rolling, would alter the condition of the material and thin it unevenly. Concurrent with these serrations, the load increased as the die-contact area increased due to the oval edges of the specimens (Fig. 2). We believe the drop in stress at the final stages is due to multiple unstable fracture of the material at the shear bands under the dies.

Because of the required higher cooling rates for glass formation, metallic glasses are necessarily prepared in the form of thin foils or ribbons. This limits the direct deformation resistance probes to the tension test, except for some palladium base glasses

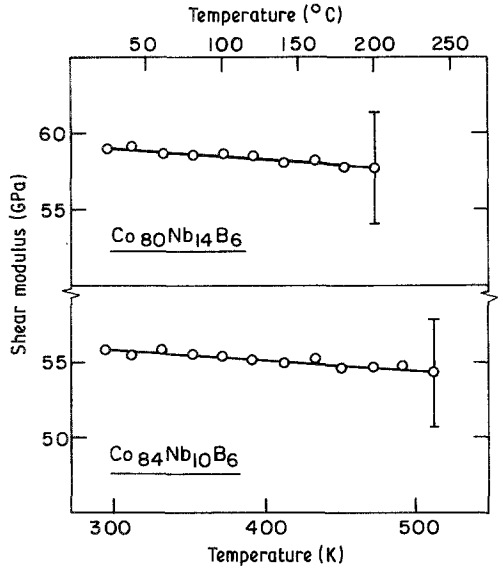

Figure 10 Shear moduli of the $Co_{80}Nb_{14}B_6$ and $Co_{84}Nb_{10}B_6$ glassy alloys as a function of temperature. No detectable changes in the moduli were observed during cooling (cycling) in this temperature range.

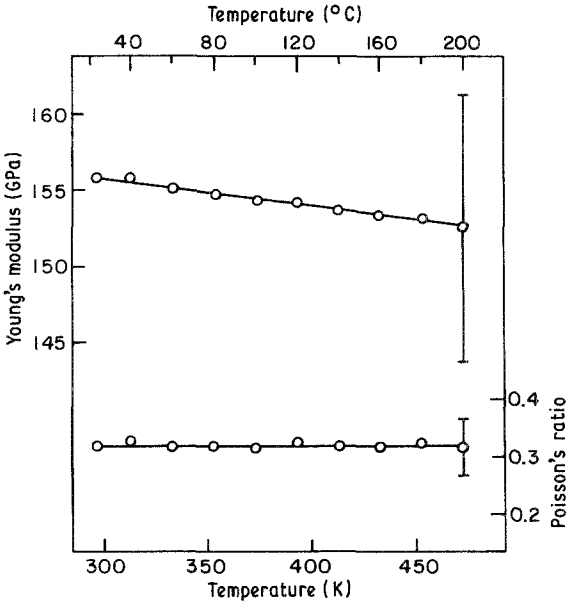

Figure 11 Young's modulus and Poisson's ratio of the $Co_{80}Nb_{14}B_6$ glass as a function of temperature.

[20]. Plane-strain compression testing, used widely in mechanical characterization of crystalline metals, particularly in simulating bulk forming processes, provides an excellent alternative for the testing of glassy alloys. In tension experiments, the stress drop due to shear band formation cannot be observed because such localizations usually lead to unstable shearing-off. In plane-strain compression, on the other hand, we have observed an increase in amplitudes of the serrations from $\sim 1\%$ of the applied load at room temperature to $\sim 5\%$ of the applied load at 473 K, and plastic strains of up to 25%. Thus, the plane-strain compression test provides a new testing technique to study the serrated plastic flow in amorphous ribbons, e.g. as a function of temperature and strain rate. This will be the subject of a separate investigation.

According to a micromechanical modelling of inelastic flow in metallic glasses based on transition state theory [8], the ratio of the plastic resistance in shear to the shear modulus was taken to be 3×10^{-2} on the basis of atomistic modelling. For an ideal plastic solid, $\tau_y = 0.57\sigma_y$, where τ_y and σ_y are plastic resistances in shear and tension, respectively. With a measured $\sigma_y = 3.01$ GPa for the Co_{80} glass, we have $\tau_y = 1.72$ GPa. From Fig. 10, the shear modulus at room temperature for this alloy is obtained as 59.0 GPa. For the Co_{84} glass, the measured hardness is 8.65 GPa. Since for an ideal plastic solid, the ratio of shear yield stress to Vicker's hardness is 0.192, we have $\tau_y = 1.66$ GPa for the Co_{84} glass. From Fig. 10, the shear modulus for this alloy at room temperature is in turn obtained as 55.8 GPa. From these values of shear strengths and moduli, we find the ratio of plastic resistance in shear to shear modulus as 2.92×10^{-2} and 2.97×10^{-2} for the Co_{80} and Co_{84} glasses, respectively. These are in excellent agreement with the earlier theoretical considerations [8].

In the presence of flow dilations, deformation resistance should be pressure dependent in metallic glasses.

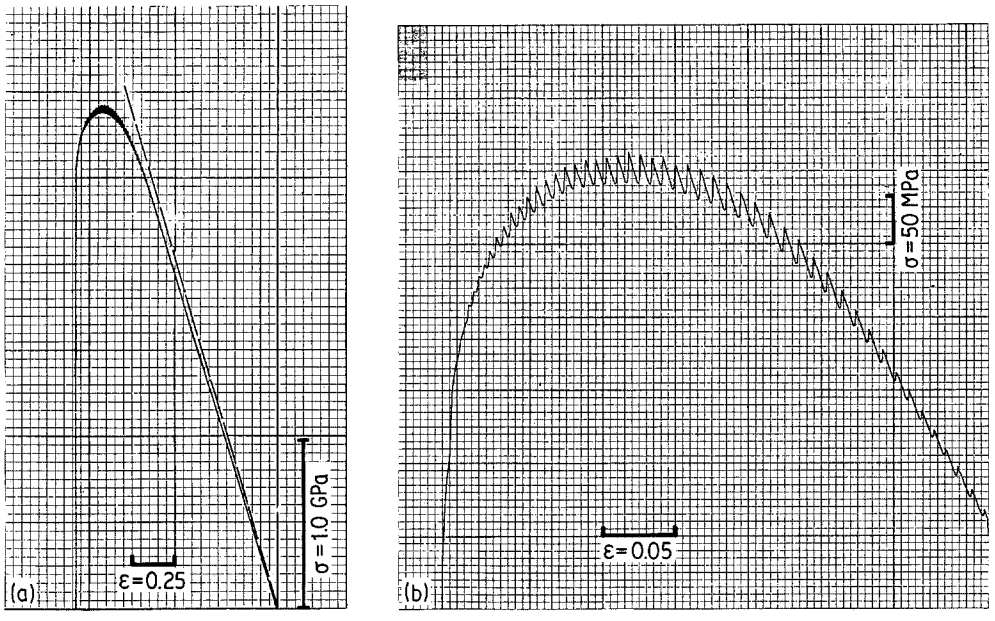

Figure 12 (a) Chart recording of the load–displacement curve for the $Co_{80}Nb_{14}B_6$ glass in plain-strain compression, at 295 K. Machine compliance is shown by the broken line. (b) Chart recording of the serrated region.

Since plastic resistance is proportional to shear modulus, and the shear modulus is pressure-dependent, a dependence of plastic resistance on the mean normal stress (negative pressure) prevalent in the chosen test is expected. Assuming a pressure dependence of shear modulus of $d\mu/dp = 0.1$, a pressure dependence of plastic resistance in shear of $dT/dp \sim 0.003$ is predicted [21]. In the present case, the excellent agreement of the ratio of plastic shear resistances obtained from hardness and plane-strain compression tests to measured shear moduli, and the relatively weak dependence of shear resistance on pressure, indicate that the observed 5% difference in plastic resistance in shear and plane-strain compression cannot be explained solely on the basis of a strength differential. We believe the difference in plastic resistance in tension and plane-strain compression is largely due to the premature failure of the material in tension caused by shear localization, and unstable shearing-off.

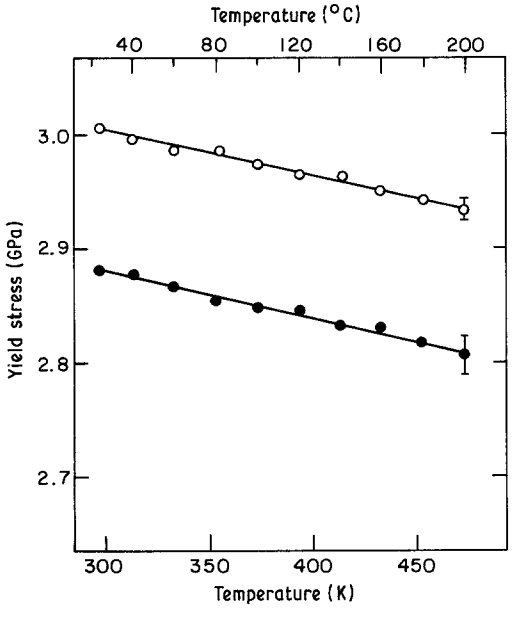

Figure 13 Yield stress of $Co_{80}Nb_{14}B_6$ glassy ribbons as a function of temperature, in plane-strain compression and simple tension. ○, Plane-strain compression; ●, simple tension.

The monotonic temperature dependent decrease of yield stress between room temperature and 473 K indicates that no transformation plasticity occurred in the $Co_{80}Nb_{14}B_6$ glass. From the flat behaviour of the internal friction spectrum, the monotonic decrease in plastic resistance, and lack of anomalies in heat evolution or absorption by DSC measurements in the temperature range 295 to 473 K, there is no evidence of any unusual behaviour in these metallic glasses, suggesting the presence of martensitic type transformations that are initiated by chemical free energy change.

Our best explanation for the phenomenon observed by O'Handley and co-workers is that it is a magnetoelastic phenomenon associated with reversible magnetization and demagnetization. Whether or not it involves small domain wall reordering would require a more detailed investigation of the magnetic nature of the phenomenon, which is worthy of a separate investigation.

6. Conclusions

1. The $Co_{80}Nb_{14}B_6$ and $Co_{84}Nb_{10}B_6$ glasses exhibit an internal friction behaviour common to many other metallic glass systems: the logarithmic decrements remain constant up to $T_c - 200$ K (or $T_g - 200$ K, whichever comes first), followed by a near exponential increase up to T_c. Ageing or increasing the oscillation frequency shifts the internal friction curve to higher temperatures, decreasing the internal friction in the temperature range $T_c - 200$ K to T_c. In the two cobalt-base glasses studied, applied saturation magnetic fields were found to have no effect on internal friction or shear modulus (no ΔE effect).

2. No evidence for transformation plasticity was found in these glasses, as internal friction scans show no peak(s), DSC shows no heat evolution or absorption, and the temperature dependence of the flow stress in the Co_{80} glass does not exhibit a discontinuous

behaviour characteristic of stress assisted martensitic transformations. Thus, the reversible thermomagnetic hysteresis observed by O'Handley and co-workers cannot be explained by martensitic transformations driven by chemical free energy change, but could instead be associated with magnetization phenomena involving magnetic domain wall motion.

3. The plane-strain compression test, devoid of premature failure, and capable of detecting shear band initiated serrated flow up to large nominal strains ($\sim 25\%$) is a new test technique to investigate the mechanical behaviour of metallic glass ribbons, which otherwise could not be studied.

Acknowledgements

This research was supported in part by the US Department of Energy, under Contract DE-AC02-83-ER45029. Turgay Ertürk was the recipient of a visiting faculty fellowship from the Allied Corporation, Morristown, New Jersey, for which we are grateful to Dr Lance Davis. We would like to express our appreciation also to Dr R. C. O'Handley for the supply of the glassy ribbons, and to Drs G. B. Olson, M. Grujicic, and J. Megusar, for useful discussions.

References

1. G. B. OLSON, in "Deformation, Processing, and Structure", edited by G. Krauss (American Society for Metals, Metals Park, Ohio, 1984) p. 391.
2. B. W. CORB, R. C. O'HANDLEY, J. MEGUSAR and N. J. GRANT, *Phys. Rev. Lett.* **51** (1983) 1386.
3. R. C. O'HANDLEY, B. W. CORB, and N. J. GRANT, *J. Appl. Phys.* **55** (1984) 1808.
4. R. C. O'HANDLEY, B. W. CORB, J. MEGUSAR and N. J. GRANT, *J. Non-Crystalline Solids*, **61–62** (1984) 773.
5. R. C. O'HANDLEY and N. J. GRANT, unpublished work (1985).
6. *Idem*, in "Rapidly Quenched Metals, Vol. II", edited by S. Steeb and H. Warlimont (North Holland, Amsterdam, 1985) p. 1125.
7. B. W. CORB, R. C. O'HANDLEY and N. J. GRANT, *ibid.* p. 1247.
8. A. S. ARGON, *Acta Metall.* **27** (1979) 47.
9. G. B. OLSON and M. COHEN, *J. Less-Common Metals* **28** (1972) 107.
10. I. TAMURA, T. MAKI, H. HATO, Y. TOMOTA and M. OKADA, in "Proceedings 2nd International Conference on Strength of Metals and Alloys, Vol. III", (Asilomar, CA, 1970) p. 894.
11. J. R. C. GUIMARAES, J. C. GOMES and M. A. MEYERS, *Supp. Trans. Jpn Inst. Met.* **17** (1976) 411.
12. G. B. OLSON and M. AZRIN, *Met. Trans.* **9A** (1978) 713.
13. T. ERTÜRK and J. C. SHYNE, *J. Iron Steel Inst.* **211** (1973) 512.
14. T. EGAMI and V. VITEK, in "Amorphous Materials: Modeling of Structure and Properties", edited by V. Vitek (TMS-AIME, New York, 1983) p. 127.
15. M. GRUJICIC, J. MEGUSAR and T. ERTÜRK, *Int. J. Rapid Solidification*, in press.
16. S. H. WHANG, L. T. KABACOFF, D. E. POLK and B. C. GIESSEN, *Met. Trans.* **10A** (1979) 1789.
17. J. MEGUSAR, A. S. ARGON and N. J. GRANT, *Mater. Sci. Eng.* **38** (1979) 63.
18. W. A. BACKOFEN, "Deformation Processing" (Addison Wesley, Reading, MA, 1972) Ch. 7.
19. N. MORITO and T. EGAMI, *Acta Met.* **32** (1984) 603.
20. C. A. PAMPILLO and H. S. CHEN, *Mater. Sci. Eng.* **13** (1974) 181.
21. A. S. ARGON, in "Rapidly Quenched Metals, Vol. II", edited by S. Steeb and H. Warlimont (North Holland, Amsterdam, 1985) p. 1325.

Received 30 May
and accepted 18 August 1986